NASA Contractor Report 3108

An Improved Supersonic, Three-Dimensional, External, Inviscid Flow Field Code

Frank Marconi and Frank Koch

CONTRACT NAS1-14162
MARCH 1979

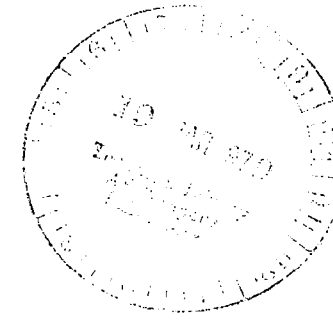

NASA

NASA Contractor Report 3108

An Improved Supersonic, Three-Dimensional, External, Inviscid Flow Field Code

Frank Marconi and Frank Koch
Grumman Aerospace Corporation
Bethpage, New York

Prepared for
Langley Research Center
under Contract NAS1-14162

National Aeronautics
and Space Administration

**Scientific and Technical
Information Office**

1979

TABLE OF CONTENTS

LIST OF ILLUSTRATIONS

SUMMARY

A numerical procedure has been developed to compute the inviscid super/hypersonic flow fields about complex vehicle geometries accurately and efficiently. A second-order accurate finite difference scheme is used to integrate the three-dimensional Euler equations in regions of continuous flow, while all shock waves are computed as discontinuties via the Rankine-Hugoniot jump conditions. Conformal mappings are used to develop a computational grid. The effects of blunt nose entropy layers are computed in detail. Real gas effects for equilibrium air are included using curve fits of Mollier charts. All of the aforementioned procedures are reported in detail in Ref. 1, and the resulting computer code is documented in Ref. 2. This report deals only with modifications to these procedures in four specific areas: inlet mass ingestion, subsonic axial Mach number, improved conformal mappings, and vehicles flying at yaw. In each area both the modifications to the computational procedures and computer code are discussed.

INTRODUCTION

The prediction of the steady three-dimensional inviscid flow fields about advanced supersonic vehicles is of great interest to the designer. Most data necessary to develop a high-speed vehicle are presently obtained from wind tunnel tests which are expensive, slow, and sometimes inadequate. The goal of this work was to create a computer code to be used to supplement experimental data in the development of high-speed vehicle configurations. This code should meet three basic requirements. The first is applicability. To obtain the required accuracy in computing the flow over a wide variety of geometries for a wide range of Mach numbers and angles of attack, the Euler equations must be solved. Small perturbation techniques yield accurate results only for the flow over slender bodies flying at low supersonic Mach numbers and small angles of attack, while Newtonian theory yields useful results only for large Mach numbers. Neither of these theories can yield all the details of the flow even over their particular range of applicability.

The second requirement is efficiency. The calculation of the flow field over a complete vehicle should take no longer than two hours on the CDC 6600 computer. This requirement can only be met by reducing the number of mesh points needed to obtain an accurate solution and keeping the program logic as simple as possible. Computational techniques that "capture" the shocks in the flow field require too many mesh points to obtain acceptable results (Ref. 3). The three-dimensional method of characteristics is rejected because of its extreme complexity in program logic.

The last requirement is that the code should be a user-oriented tool. This is in contrast to codes that are tailor-made for a particular configuration (Ref. 4), and codes that must be constantly monitored "to nurse the solution through critical regions" (Ref. 5). The designer should only have to specify the vehicle geometry and flight conditions to obtain reliable results in a directly usable form (aerodynamic coefficients, boundary layer inputs, etc.). The vehicle geometry should be input via techniques that, on the one hand, are of the same level of advancement as those used in the best incompressible, supersonic and hypersonic three-dimensional tools, and, on the other hand, posses longitudinal and cross-sectional continuity needed when solving partial differential equations. The geometry package of Ref. 6 was used to meet these requirements.

The general numerical scheme used to solve this problem has been developed by Moretti (Refs. 7-10). It follows a number of basic guidelines:

- A second-order accurate finite difference marching technique (satisfying the CFL stability condition) is used to integrate numerically the governing partical differential equations
- All shock waves in the flow field are followed, and the Rankine-Hugoniot conditions are satisfied across them
- The intersection of two shocks of the same family is computed explicitly
- Conformal mappings are used to develop a computational grid
- The body boundary condition is satisfied by recasting the equations according to the concept of characteristics

- The edge of the entropy layer on blunt nose vehicles is followed from its origin, and special devices are used to form derivatives across it
- Real gas effects are included (equilibrium air) when appropriate by using curve fits of Mollier charts
- Sharp leading edges on wing are computed using a local two-dimensional solution

The details of all of these procedures are discussed in Ref. 1. This report discusses a number of advances to the methods of Ref. 1:

- A procedure for including the effects of intake installations on external flow fields
- A scheme for integrating through a region in the flow field where the total Mach number is supersonic while its component in the marching direction is subsonic
- A new conformal mapping procedure
- The ability to compute the flow about a vehicle when the free stream velocity vector is not contained in the geometric symmetry plane

All of these advances are discussed in detail. In addition, typical results are shown and all code modifications listed.

INLET MASS INGESTION

Computational Procedure

In this area the intent was to include the effect of a flow through inlet system on the vehicle flow field. The inlet face is assumed to be planar and normal to the marching direction. The calculation proceeds by marching to the inlet station where the geometry cross-section jumps from the cross-section without the inlet to the cross-section with the inlet. The cross-sectional flow field data are interpolated onto the grid bounded by the

cross-section with the inlet. In addition, the velocity directions on the body are changed to match the new body boundary conditions.

Typical Results

Figure 1a is a comparison of the shock patterns on an aircraft configuration with an inlet and the same configuration with its under surface faired from the nose to the inlet face. There is an additional shock generated by the inlet lower lip. Figure 1b shows the corresponding under surface, symmetry plane pressure distribution.

Code Modifications

The geometry code being used did not have to be changed to include the inlet mass ingestion capability. The flow field code (STEIN) requires only the position of the inlet station (ZINLET) as additional data. This quantity is read at the end of the second input card. If the configuration under consideration does not have an inlet, this quantity should be set to a station before the starting station.

SUBSONIC AXIAL MACH NUMBER

Computational Procedure

The only inherent limitation in a marching technique like the one of Ref. 1 is that the Mach number component in the marching direction (Fig. 2) must be supersonic. As an illustration of the limitations of a standard marching technique, Fig. 3 shows regions of applicability of a standard marching for a circular cone (marching direction is the cone axis). In the computation of three-dimensional flow fields, regions of subonic axial and supersonic total Mach number have been encountered quite often. The procedure, which was developed to integrate through regions of subsonic axial Mach number, is reported in detail in Ref. 11. The scheme basically involves marching in a rotated direction, to preserve the proper domain of dependence of each computational grid point. Figure 4a shown a group of grid points in the X, Z plane (X is a coordinate measured normal to the body; X = 0 is the body; Z is the marching direction). The data at Z_0 (points A', B', C', D'

are given) and the data at $Z_0 + Z$ are to be found. Shown in the figure are the down-running characteristics (dotted lines) at $Z_0 + \Delta Z$. At point C, the down-running characteristic moves ahead of the plane $(Z_0 + \Delta Z)$, so that information from ahead of this plane (i.e., point E) must be allowed to affect point C. This grid point is typical of a subsonic axial Mach number point. The grid point B has a supersonic axial Mach number and can be computed with a standard marching technique. In addition, the boundary point A can be computed with a standard marching technique. The grid point D has a near sonic axial Mach number so that for efficiency it can be computed with the subsonic axial Mach number scheme. At the points C and D a rotated coordinate system ($\xi = X$ and $\eta = X + \alpha Z$, $\alpha = \Delta X/\Delta Z$) is used (Fig. 4b). The procedure implicitly marches from one η = constant plane to the next with difference equations:

$$F_\xi \simeq (F_{N+1,\,K-1} - F_{N-1,\,K+1})/2\Delta X$$

$$F_\eta \simeq (F_{N,K} - F_{N,K-1})/\alpha\Delta Z$$

These difference formulas are implicit since the ξ derivatives are taken at the η = constant plane of interest. In this way the proper domain of dependence of grid points is preserved. The data at a point like C depends upon the data at E (Fig. 4a).

Typical Results

To test the procedure, a problem free of complication (but having a region of subsonic Mach number in the marching direction) is chosen. The problem was that of the flow in a two-dimensional duct where the lower wall remains straight while the upper wall expands. To generate an imbedded region of subsonic Mach number in the marching direction, this direction was chosen such that there was a 50° angle between it and the initial velocity direction. Figure 5 shows the duct, marching direction, computer isobars, and the region of subsonic Mach number in the marching direction. This entire flow field was computed using the technique developed for region of subsonic axial Mach number. The dashed lines in Fig. 5 are the exact, simple wave isobars at the beginning and end of the expansion. The computed results

compare quite well with the exact solution. This problem, although somewhat trivial, proved that the procedure is stable and yields accurate results.

The second problem we applied this technique to was that of computing the flow over a blunted cone with a flare. The marching direction must be the cone axis, since the problem is symmetric about this axis. Figure 6 shows the flared portion of this geometry in addition to the shocks, isobars, and region of subsonic axial Mach number. In this computation the region of subsonic axial Mach number was computed using the technique presented here, while the surrounding flow was computed using a standard marching technique. This computation indicates that the procedure described here can be used with a standard marching technique.

Figure 7 shows the results of a computation of the flow about another blunted, flared cone. In this case, the region of subonic axial Mach number extends from the cone surface to the imbedded shock. As in the previous result, only the region of subsonic axial Mach number was computed using the new technique.

To demonstrate this procedure in three-dimensional computations, the problem of the low Mach number flow over a canopy was considered. Figure 8 shows results of this computation. The free stream Mach number is 1.7, so that the surface Mach number is about 1.6 before the canopy (Z = 8), and the compression from the canopy forces a bubble of subsonic axial Mach number. Figure 8a shows the body, canopy shock, and the region of $w < a$ in side view; Figs. 8b, c, d, and e are cross-sectional views. In this case, the bubble of subsonic axial Mach number calculation is carried out in the X-Z plane, X being the computational coordinate normal to the body.

Code Modification

The new procedure for regions of subsonic axial Mach number is automatically implemented when required. No additional input data are required.

CONFORMAL MAPPINGS

Computational Procedure

A new more powerful conformal mapping procedure has been developed by Moretti (Ref. 12), and in this work it has been applied to the code of Ref. 1. The procedure involves the repeated application of the simple Karman-Trefftz transformation.

An example of a complex vehicle cross-section in a z = constant plane is shown in Fig. 9a (dashed line). The goal of the mapping reduces to transforming this cross section into one which is more circular (Fig. 9g), so that a polar coordinate system (r,θ) can be used. To achieve this goal, the corners (points number 1-5 in Fig. 9a) in the cross section must be eliminated. In terms of complex variable $\omega = x + iy$ and $\zeta = re^{i\theta}$, a Karman-Trefftz transformation may be written:

$$\frac{\zeta-1}{\zeta+1} = \left(\frac{\omega-\omega^*}{\omega+\bar{\omega}^*}\right)^{\pi/\delta}$$

where ω^* is the complex coordinate of the corner ($\bar{\omega}^*$ is its conjugate) and δ is the internal angle of the corner. The mapping procedure simply involves the repeated application of this transformation at each corner.

It became apparent early in this work that the order in which the corners were eliminated was important. The best results were achieved if the corner with the largest external angles was mapped first. Figure 9 shows a sequence of cross sections as each corner in Fig. 9a is eliminated. Figure 9g shows the cross section after all the corners were eliminated; the final coordinate system used is polar r, θ in the ζ space.

Typical Results

Figure 10 shows the grid lines θ = constant in the physical space resulting from the use of this mapping technique for several configurations of different cross sections. The concentration of grid lines in critical regions (wing tips, etc.) is demonstrated in the figure. This concentration is required for any successful computation.

Figure 11 shows an application of these mappings to a simple conical cambered wing. The figure shows span-wise surface pressure distributions on an elliptic cone and a corresponding cambered ellipse (tip angle = -20°). The effect of spanwise cambering is to reduce the large tip expansion and therefore the subsequent recompression. This reduction is important in terms of boundary layer separation.

Figure 12 shows a series of computed cross-sectional shock patterns. The geometry was the X24C-12I large dihedral wing configuration, which required four Karman-Trefftz transformations to generate a grid.

Code Modifications

The application of this mapping procedure was not automated during the current effort. The mappings must be very closely related to the geometry definition. The geometry/mapping package has not yet been developed. The results of Fig. 12 were computed using a pilot code.

YAW

Computational Procedure

The work of Ref. 1 assumed a plane of symmetry for the flow field. Therefore, the free stream velocity vector was taken in the geometric symmetry plane. The code of Ref. 2 was modified to eliminate this restriction so that flows with the free stream velocity vector at angle β out of this geometric symmetry plane could be computed. The modification involved elimination of the symmetry conditions and the computation of both sides of the geometric symmetry plane. The only problems encountered were of a book-keeping and coding nature, so they will not be discussed here.

Typical Results

Figure 13 is a comparison of the under surface streamline patterns on the X24C-12I configuration at three yaw angles. The shifting of the confluence of streamlines with increasing β can be seen from the figure. Figure 14 shows the cross-sectional shock patterns for the X24C-12I configuration at $\beta = 5°$; the figure shows the asymmetry in the shocks.

Figure 15 is a comparison of surface pressures on the X24C-12I at $\beta = 0$ and $\beta = 5°$. At $\beta = 0$, the pressure exhibits a local maximum at the 12th grid point and an expansion at the turn on the upper portion of the cross section. At $\beta = 5°$, there is a local maximum in pressure only on the windward side of the configuration.

A configuration study was performed using the yaw capability developed during this effort. Three configurations were studied and are shown in Fig. 16. These configurations were studied primarily to determine the effects of yaw on inlet flow fields. Figure 17 presents the flow direction at the inlet face (which is essentially uniform across inlet face) versus the free stream β for all three configurations. The figure shows that the local β is smaller than the free stream value for all three configurations. Figure 18 shows the same flow direction plot, but for one configuration X24C-L16 at two different Mach numbers. Figure 19 is an attempt to show the variation of inlet Mach number with free stream Mach number for $\beta = 0°$ and $\beta = 2.5°$. The effect of β on the local Mach number is imperceptible.

Code Modifications

The computer running times and core requirements have essentially been doubled by adding this yaw capability to the code of Ref. 2. The only additional input data required are the value of the yaw angle BETA (in degrees), which is read on data card number 12. The starting solution codes (BLUNT, SHARP) have also been modified for the yaw capability, with the restriction that the starting geometry have a circular cross-section.

CONCLUSIONS

All of the modifications discussed in this report have enhanced the capabilities of the code of Ref. 1 significantly. They all represent steps toward the ultimate goal of a flow field prediction tool that can be used simply in the design of advanced vehicles.

It was proven during this work that a great deal of flexibility could be gained by using the newly developed mapping procedures of Moretti. As mentioned previously the use of these mappings requires a geometry definition package more closely tied to the mappings than presently available.

REFERENCES

1. Marconi, F., Salas, M.D., and Yaeger, L., Development of a Computer Code for Calculating the Steady Super/Hypersonic Inviscid Flow Around Real Configurations, Vol. 1 - Computational Technique. NASA CR-2675, 1976.

2. Marconi, F. and Yaeger, L.: Development of a Computer Code for Calculating the Steady Super/Hypersonic Inviscid Flow Around Real Configurations, Vol. II, Code Description. NASA CR-2676, 1976.

3. Moretti, G.: Three Dimensional, Supersonic, Steady Flows with any Number of Imbedded Shocks. AIAA Paper No. 74-10, 1974.

4. D'Attore, L., Bilyk, M.A., and Sergeant, R.J.: Three Dimensional Supersonic Flow Field Analysis of the B-1 Airplane by a Finite Difference Technique and Comparison with Experimental Data. AIAA Paper No. 74-189, 1974.

5. Kutler, P., Lomax, H, and Warming, R.F.: Computation of Space Shuttle Flow Fields Using Noncentered Finite-Difference Schemes. AIAA Paper No. 72-193, 1972.

6. Vachris, A. and Yaeger, L.: Quick-Geometry A Rapid Method for Mathematically Modeling Configuration Geometry. NASA SP-390, 1975.

7. Moretti, G., Grossman, B., and Marconi, F.: A Complete Numerical Technique for the Calculation of Three Dimensional Inviscid Supersonic Flows. AIAA Paper No. 72-192, 1972.

8. Moretti, G.: Thoughts and Afterthoughts about Shock Computations. PIBAL Report No. 72-37, 1972.

9. Moretti, G. and Pandolfi, M.: Entropy Layers, J. Computers and Fluids, Vol. 1, No. 19, 1973.

10. Moretti, G. and Pandolfi, M.: Analysis of the Inviscid Flow about a Yawed Cone (Preliminary Studies). PIBAL Report No. 72-18, 1972.

11. Marconi, F. and Moretti, G.: Three Deimsnional Supersonic Flows with Subsonic Axial Mach Numbers. AIAA Paper No. 76-383, 1976.

12. Moretti, G.: Conformal Mappings for Computations of Steady, Three-Dimensional, Supersonic Flows. Numerical/Laboratory Computer Methods in Fluid

10 Mechanics. presented at the Annual Winter Meeting of the ASME (New York), Dec. 5-10, 1976.

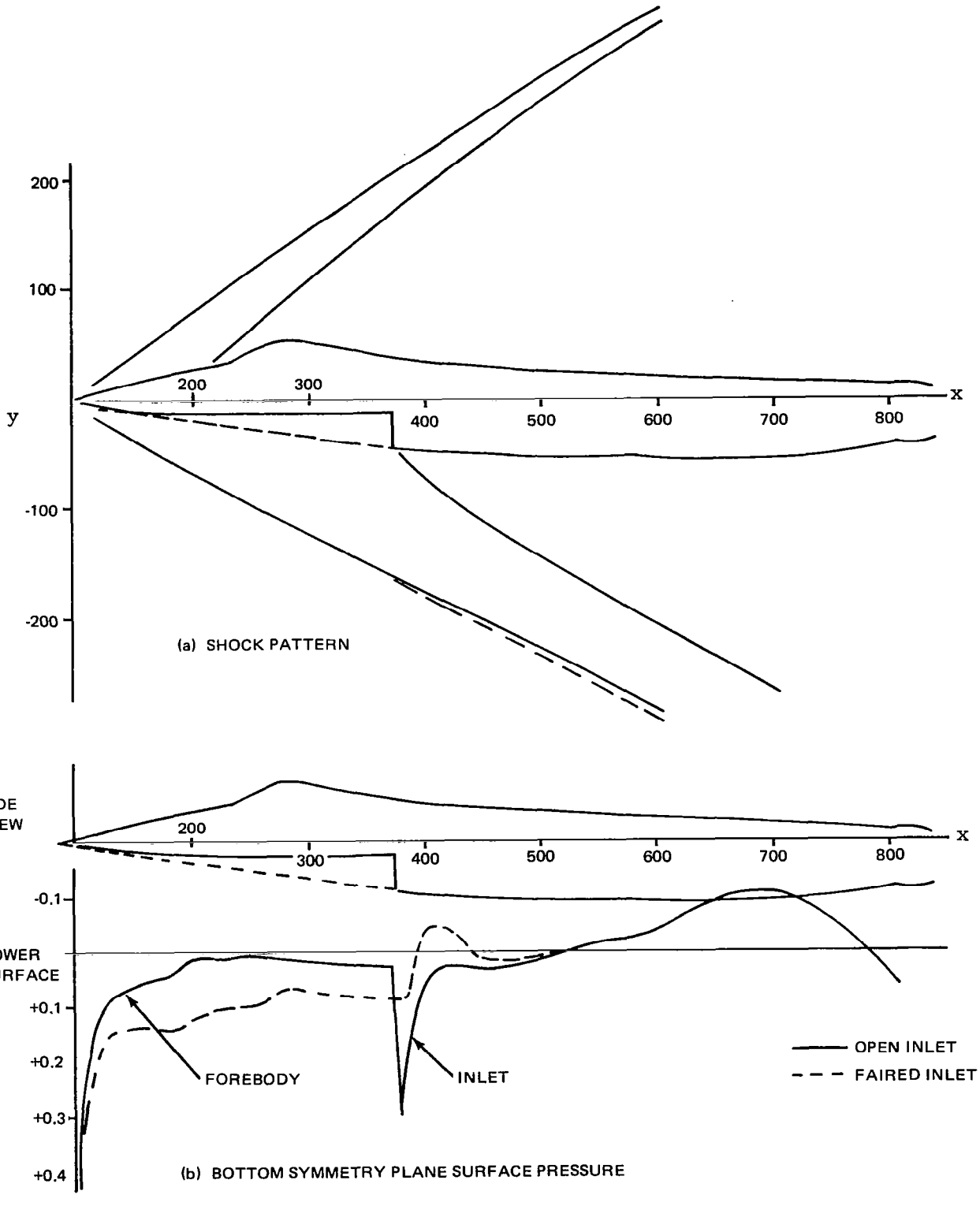

Fig. 1 Flow Field Comparison with and without Inlet ($M_\infty = 2, \alpha = 0^o$)

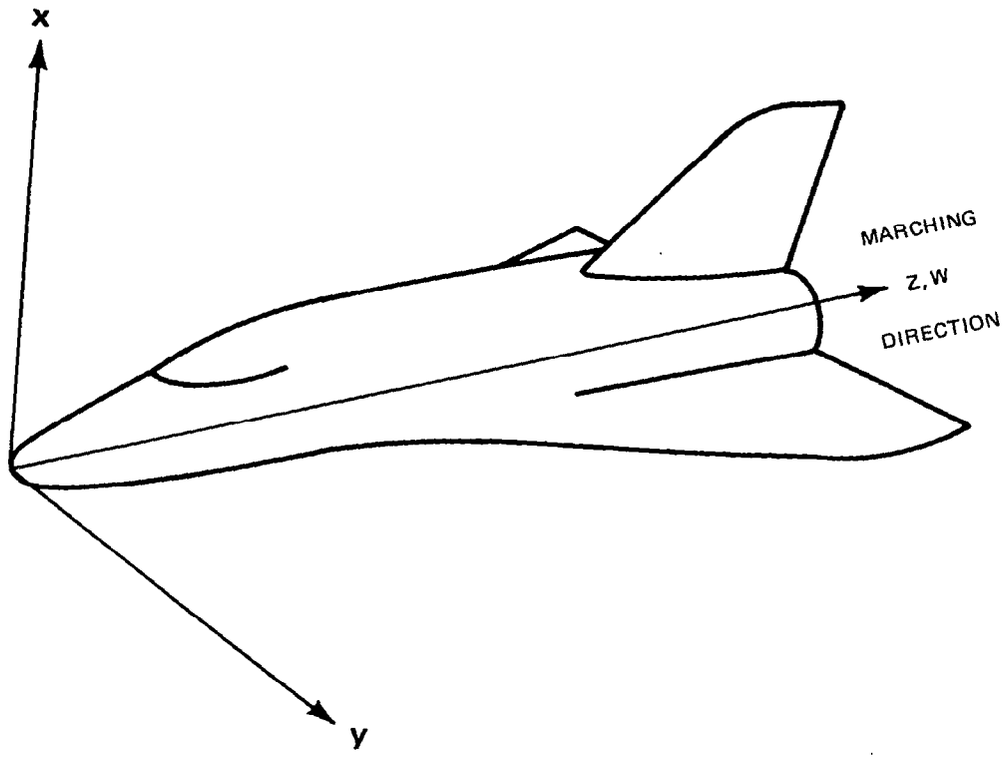

Fig. 2 Typical Configuration, Marching Direction

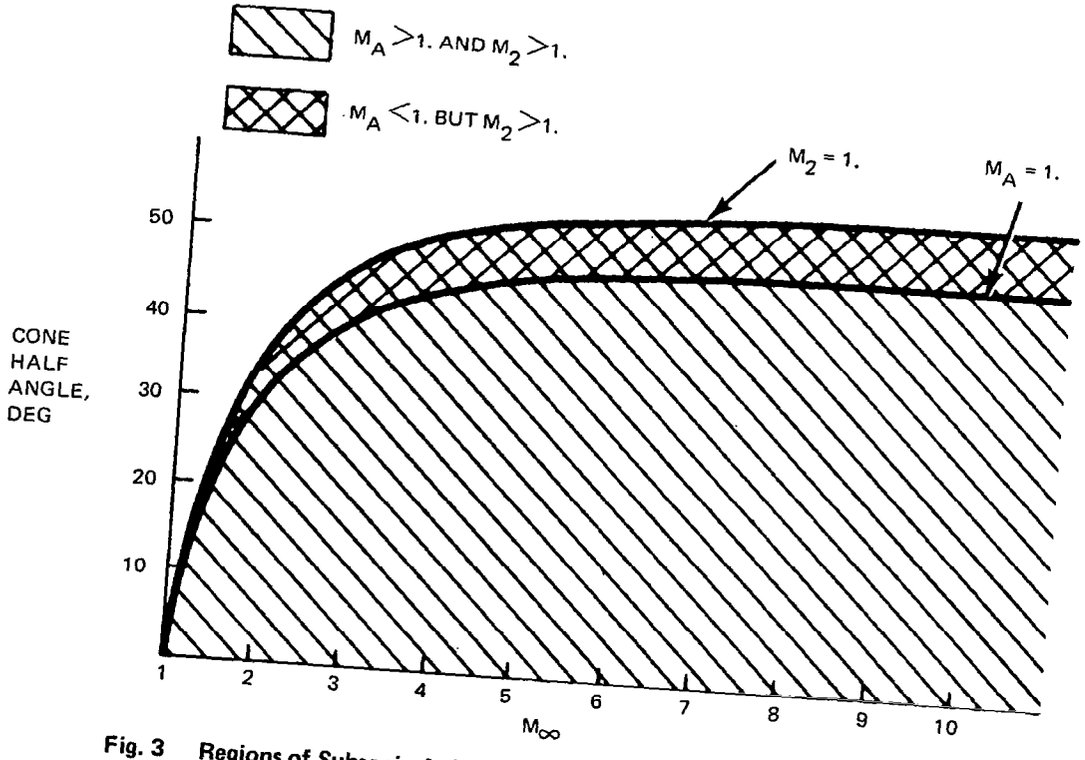

Fig. 3 Regions of Subsonic Axial Mach Number for a Cone (M_2 = Surface Mach, M_A = Axial Component)

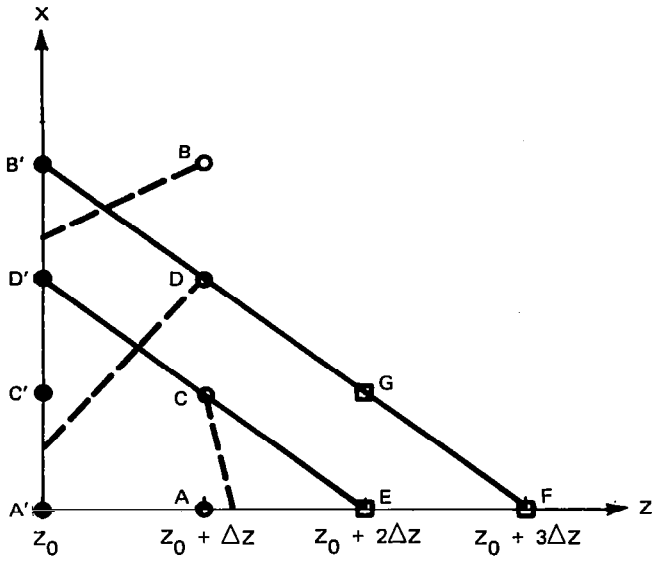

(a)

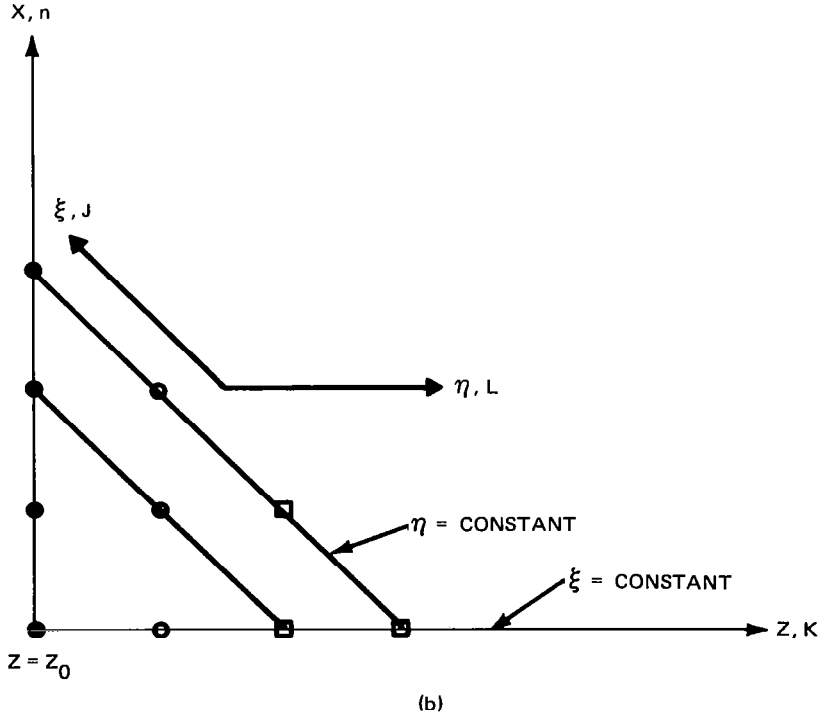

(b)

Fig. 4 Subsonic Axial Mach Number Local Coordinates

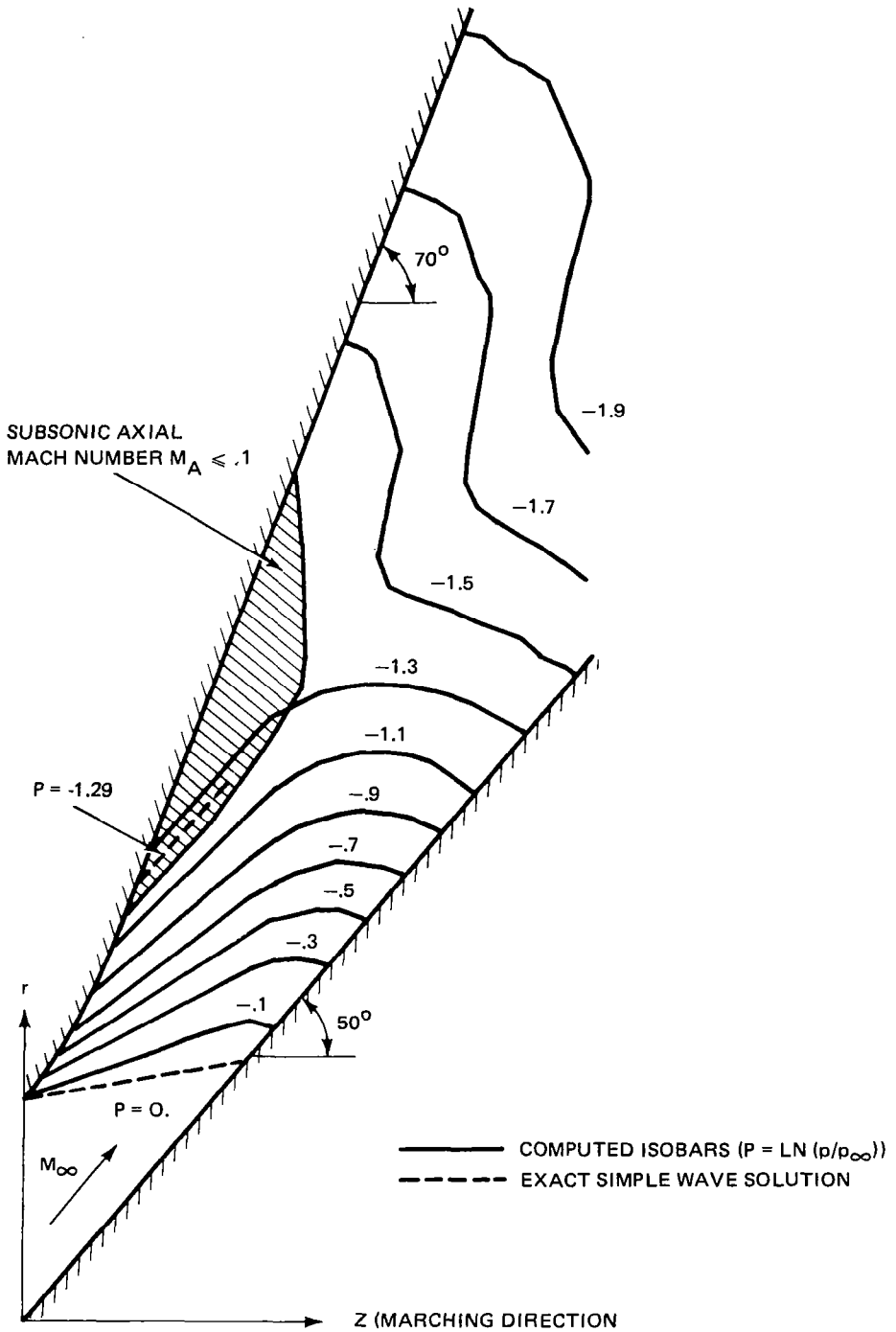

Fig. 5 Two-Dimensional Duct Flow with Subsonic Axial Mach Number ($M_\infty = 2$)

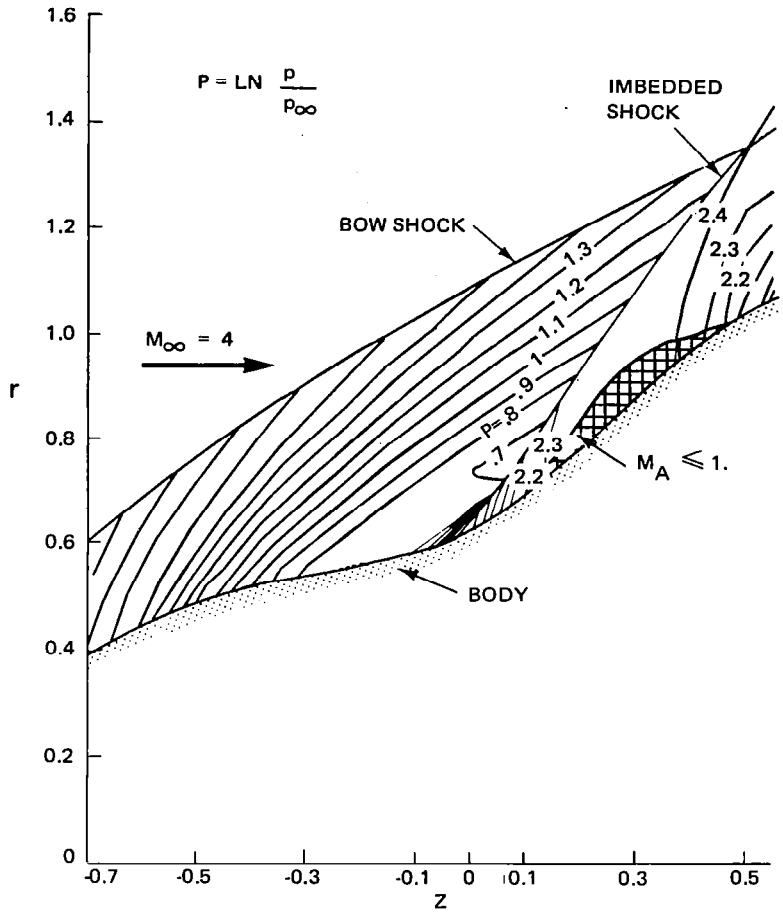

Fig. 6 Computed Isobars on a Flared Blunt Cone

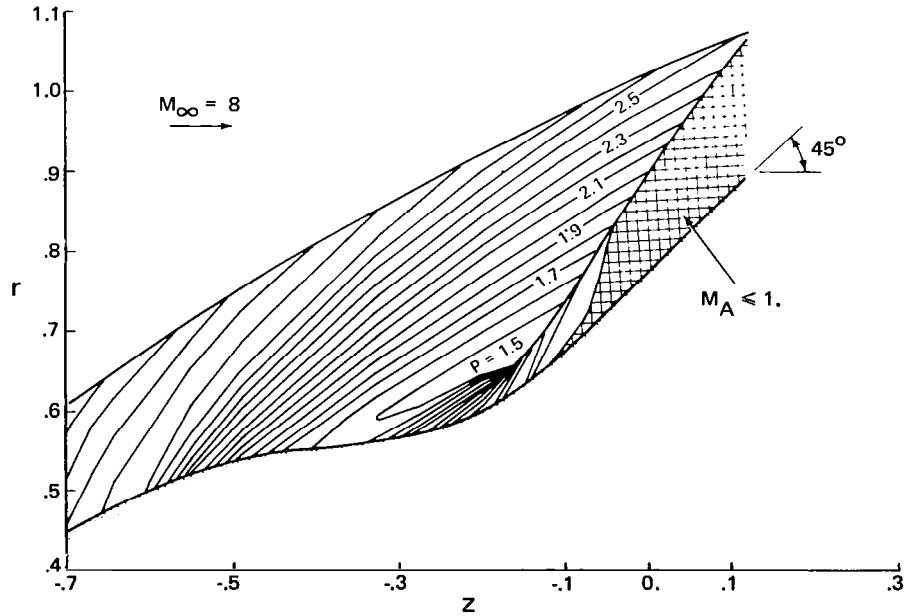

Fig. 7 Flared Cone Computation with $M_A < 1$ Behind Imbedded Shock

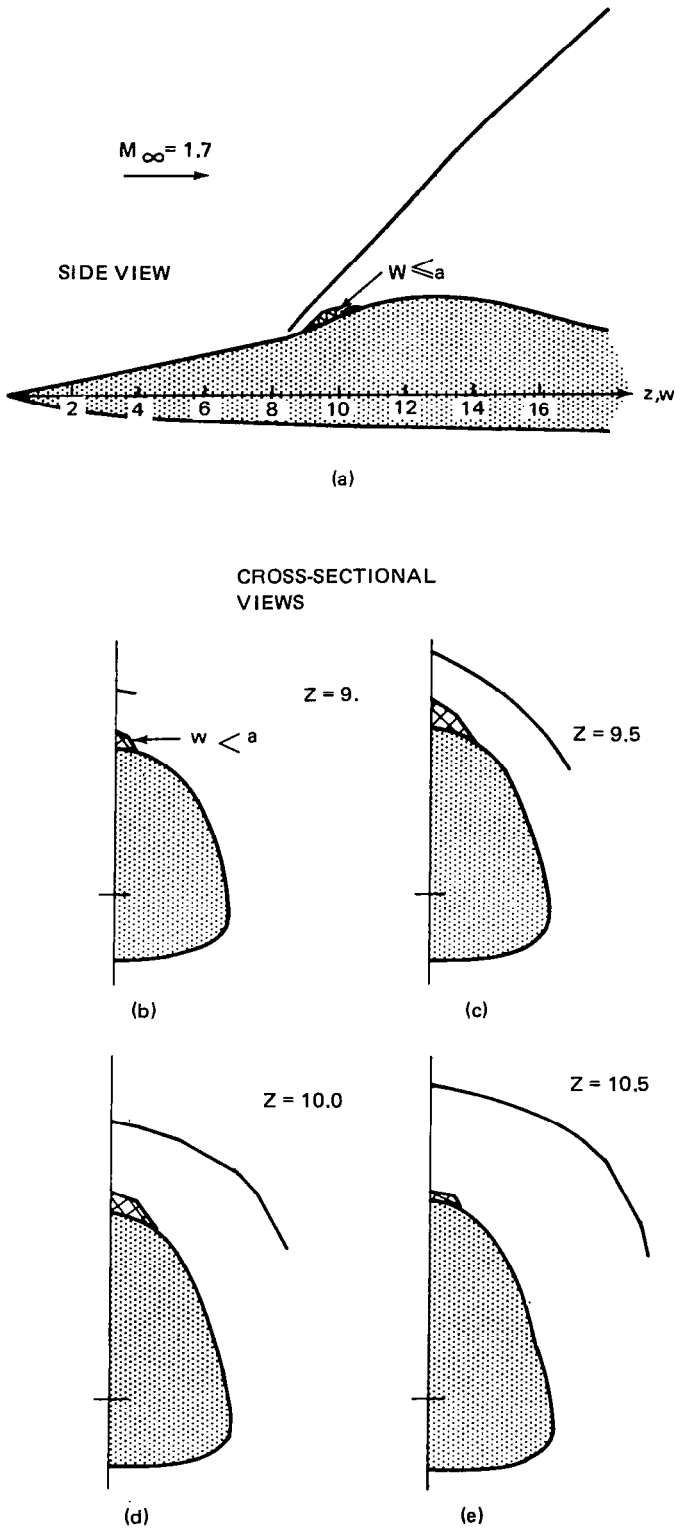

Fig. 8 Aircraft Forebody with $M_A < 1$ on the Canopy

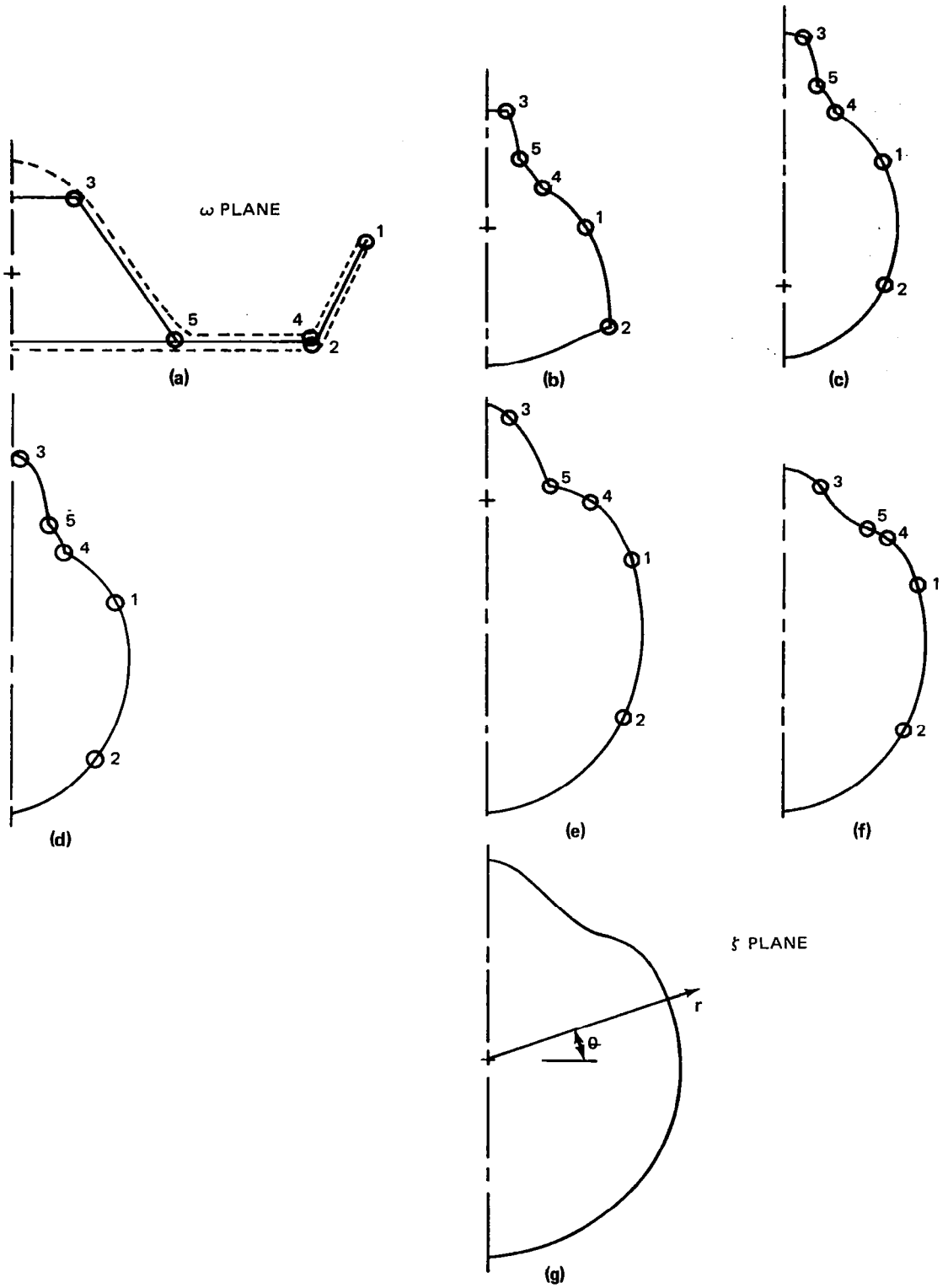

Fig. 9 Series of von Karman-Trefftz Mappings

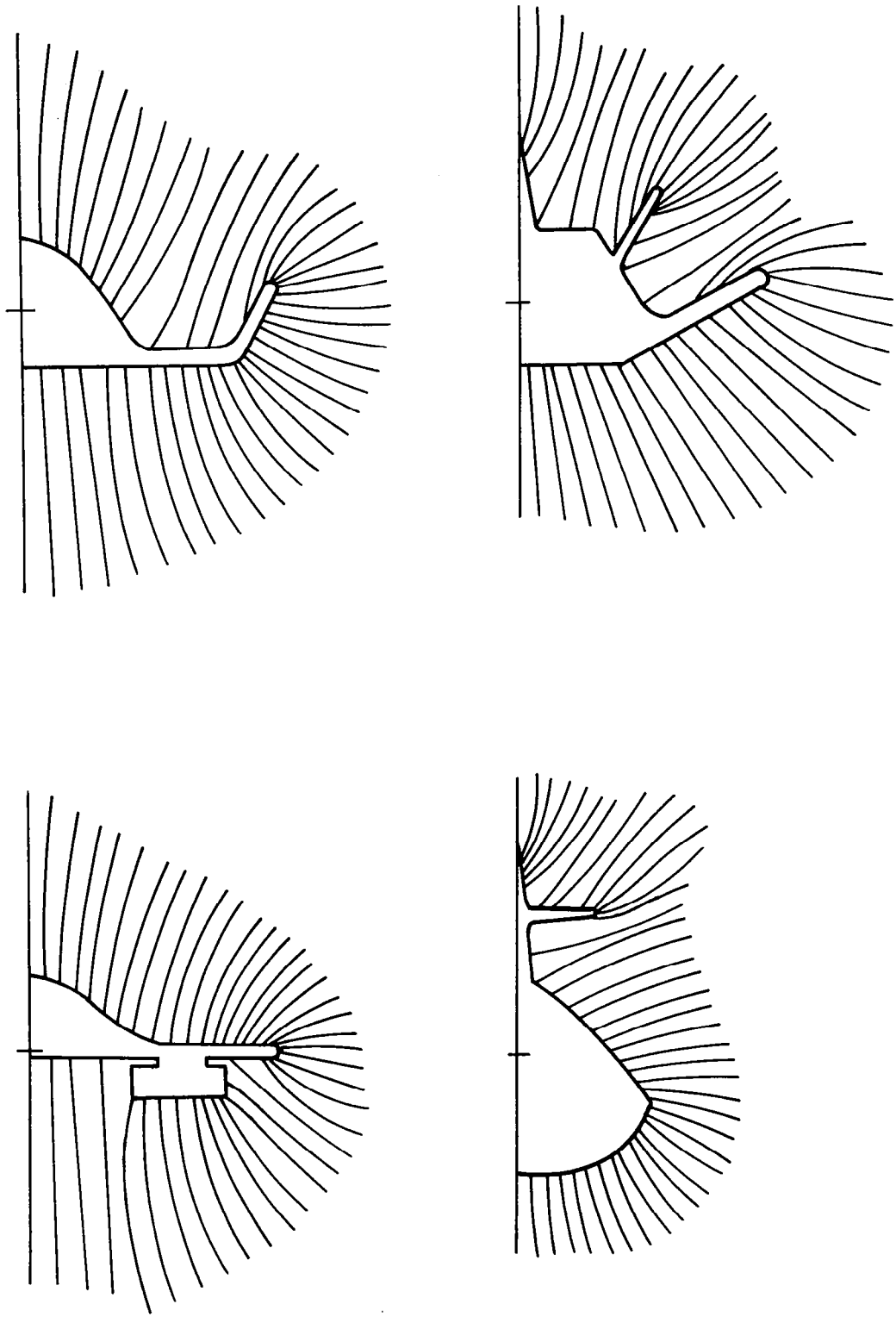

Fig. 10 Several Configurations with Grid Lines Generated with New Mappings

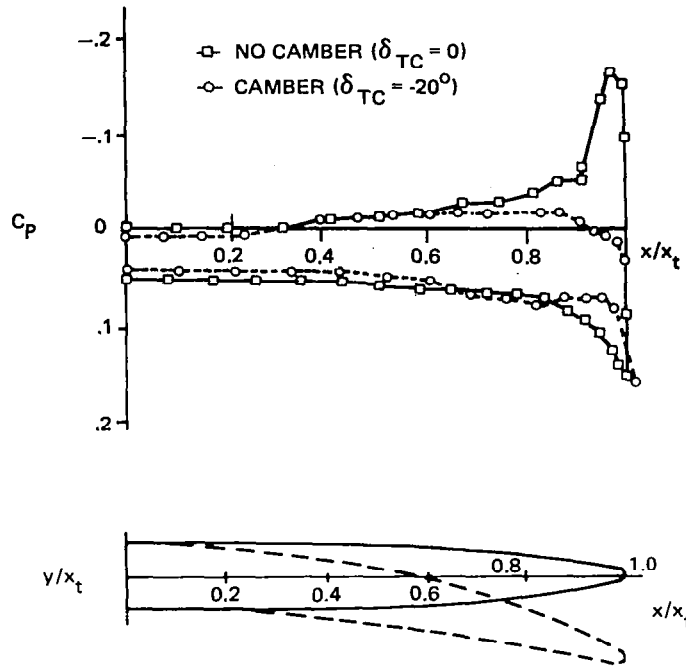

Fig. 11 Surface Pressure Comparison (14:1 Elliptical Wing $M_\infty = 2$, $\alpha = 3^o$)

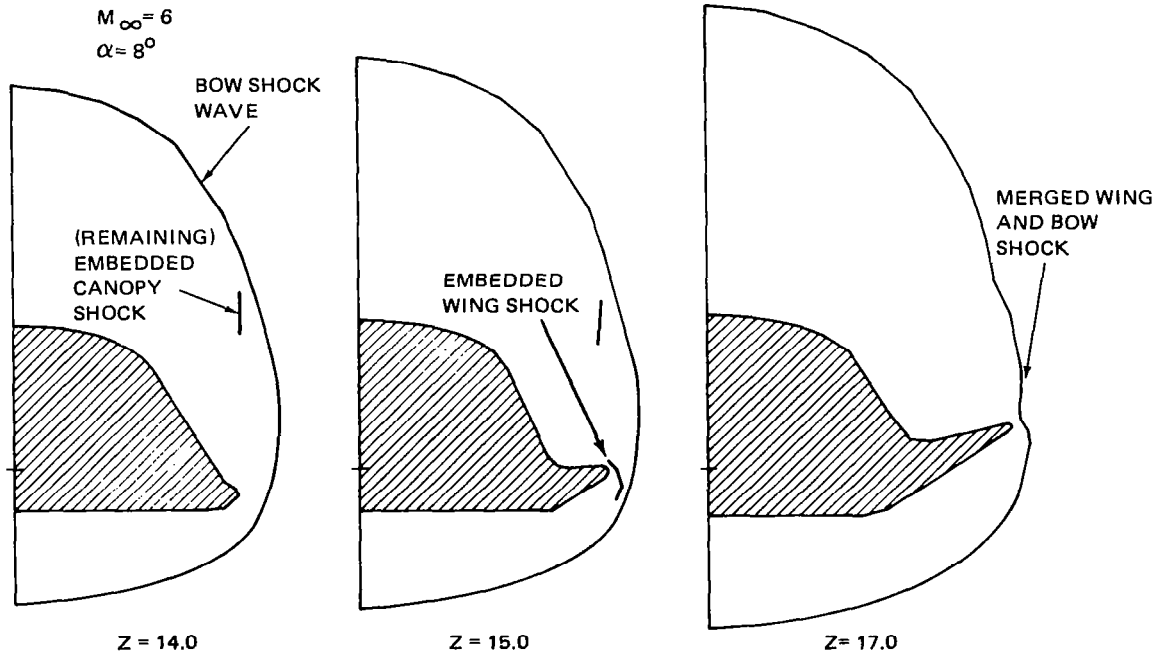

Fig. 12 X242-12I Dihedral Wing Shock Pattern

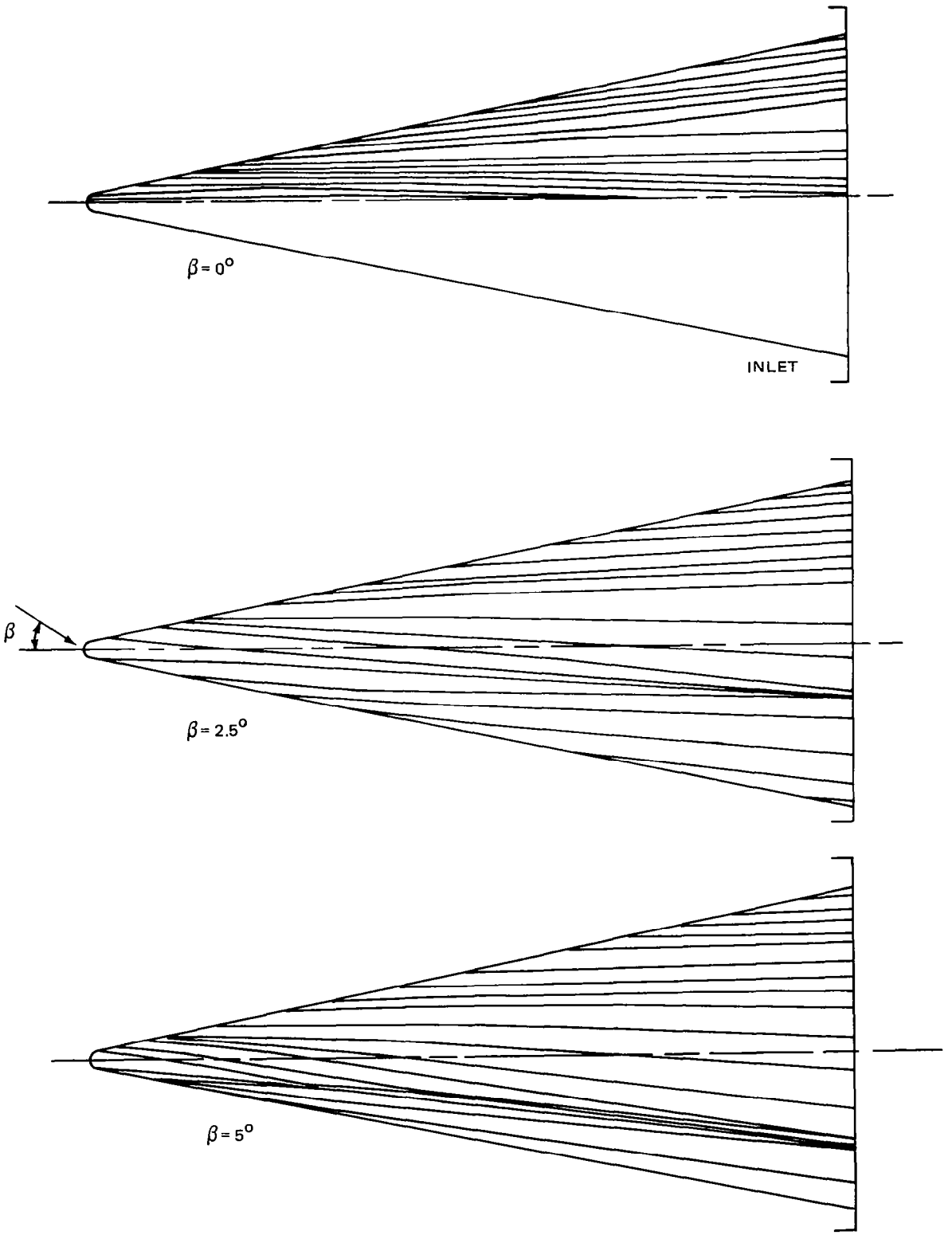

Fig. 13 Windward Surface Streamlines X24C-121, $M_\infty = 6$, $\alpha = 5^o$

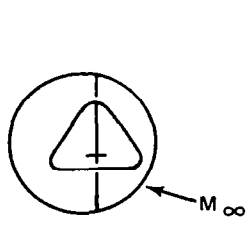

Z = 2.

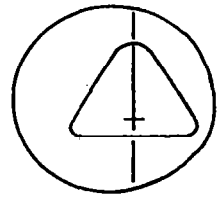

Z = 3.

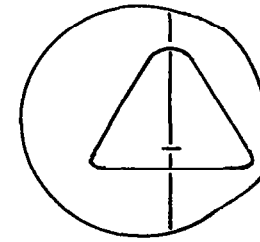

Z = 4.

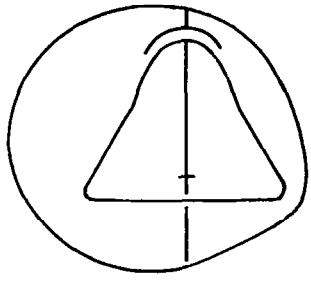

Z = 5.

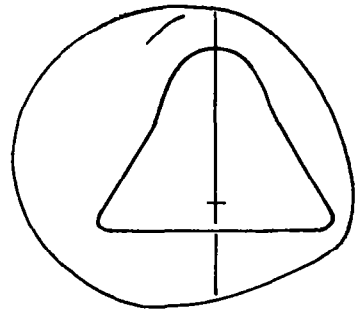

Z = 6.

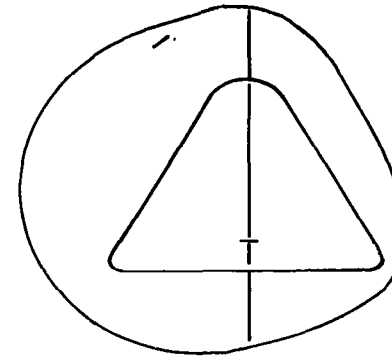

Z = 7.

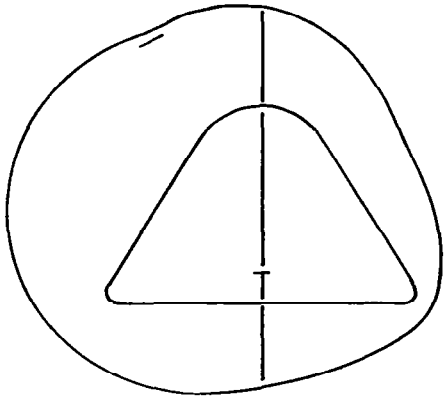

Z = 8.

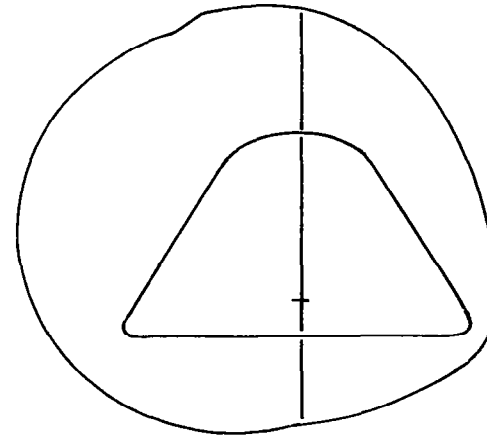

Z = 9.

Fig. 14 Cross-Sectional Shock Patterns X24C-121, $M_\infty = 6$, $\alpha = 5^o$, $\beta = 5^o$

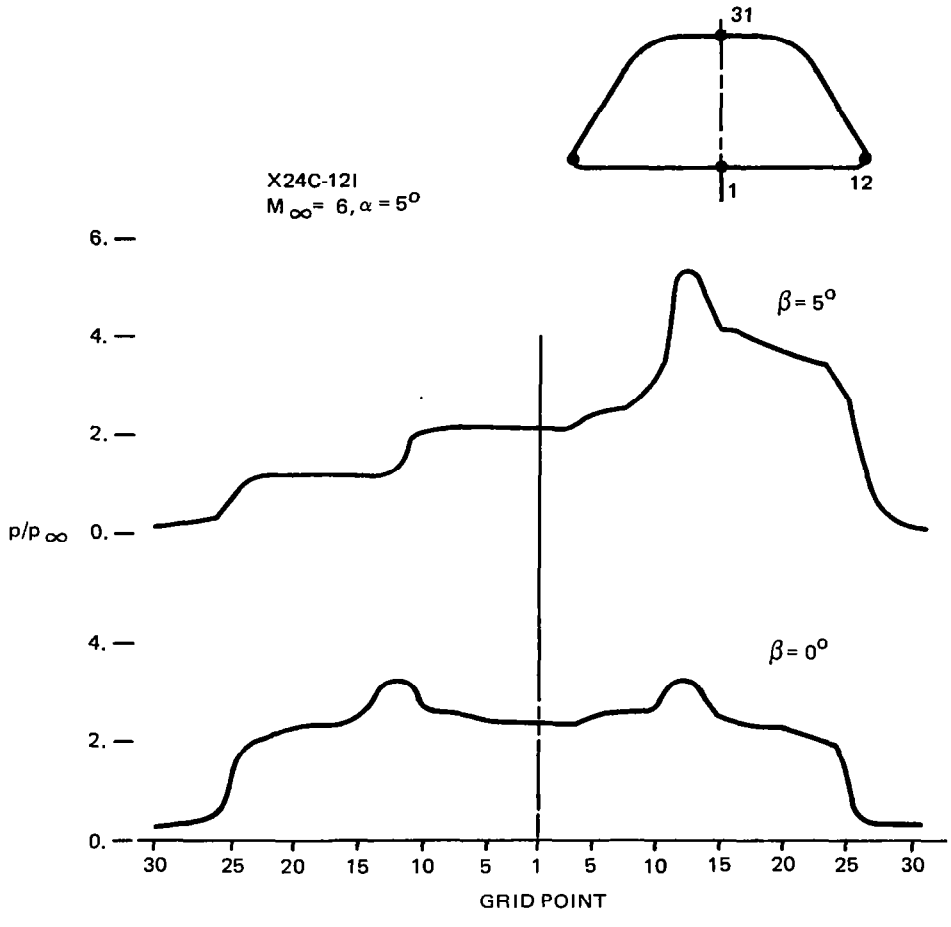

Fig. 15 Cross-Sectional Surface Pressure Distribution

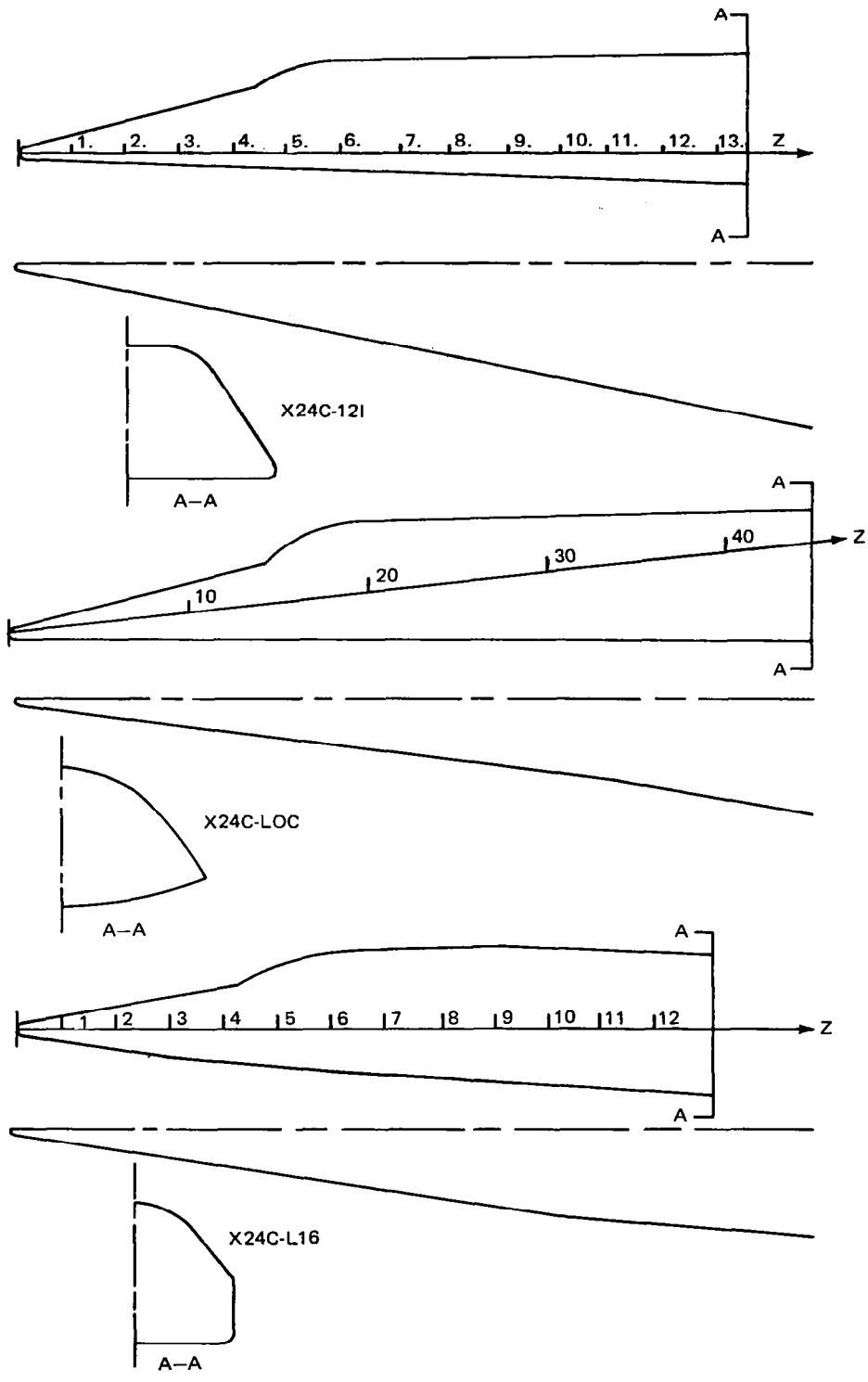

Fig. 16 Three Hypersonic Configurations to be Studied

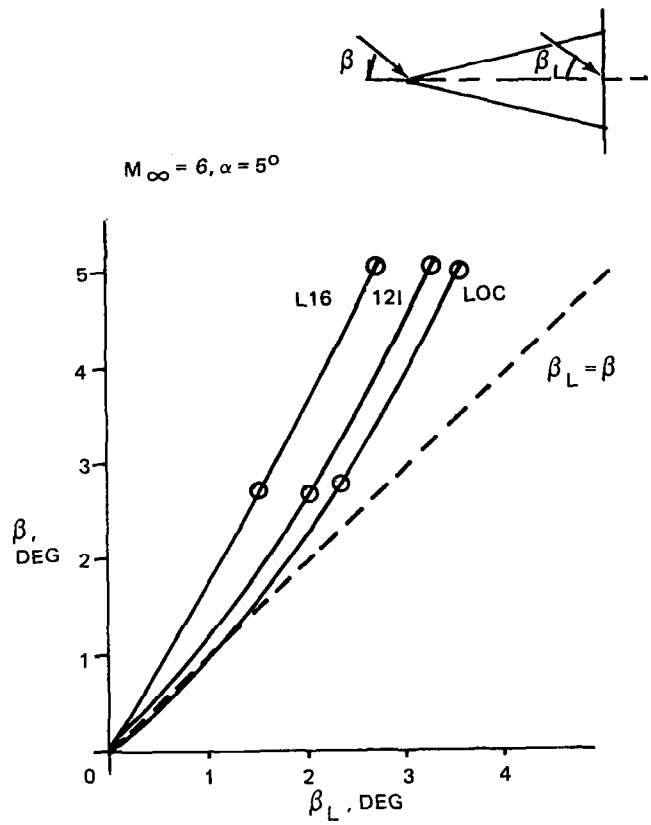

Fig. 17 Inlet Flow Direction, Three Configurations

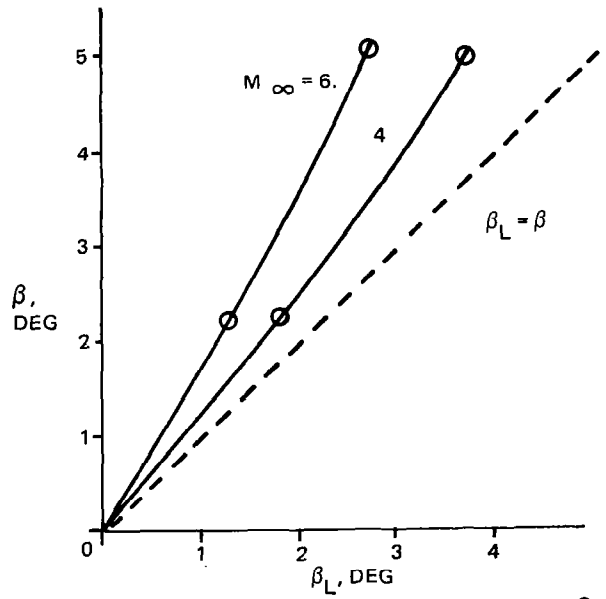

Fig. 18 Inlet Flow Direction X24C-L16, $\alpha = 5^o$

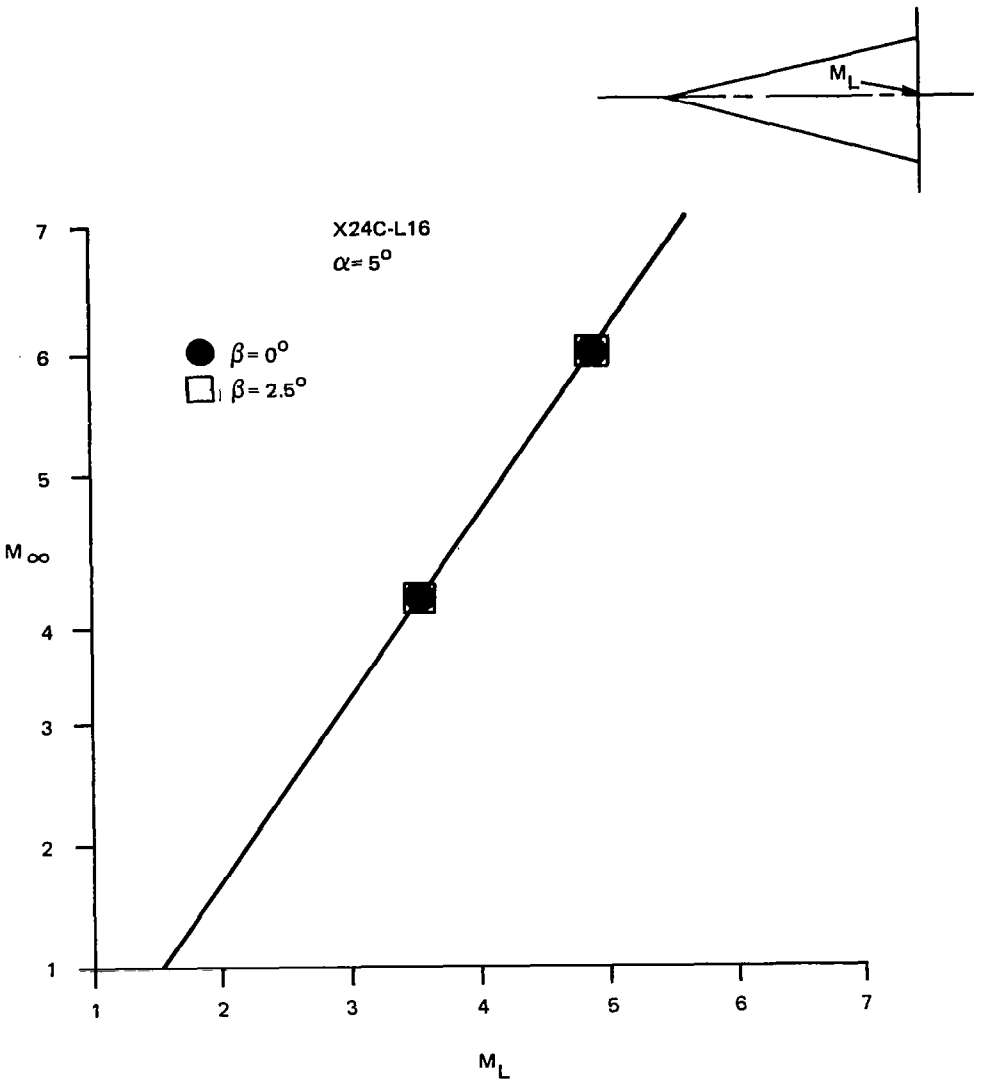

Fig. 19 Inlet Mach Number

1. Report No.	2. Government Accession No.	3. Recipient's Catalog No.
NASA CR-3108		

4. Title and Subtitle	5. Report Date
An Improved Supersonic, Three-Dimensional, External, Inviscid Flow Field Code	March 1979
	6. Performing Organization Code
7. Author(s)	8. Performing Organization Report No.
Frank Marconi and Frank Koch	
	10. Work Unit No. 505-11-31-02
9. Performing Organization Name and Address	11. Contract or Grant No.
Grumman Aerospace Corporation Bethpage, NY 11714	NAS1-14162
	13. Type of Report and Period Covered
12. Sponsoring Agency Name and Address	Contractor Report
National Aeronautics and Space Administration Washington, DC 20546	14. Sponsoring Agency Code

15. Supplementary Notes

Langley Technical Monitor: M. D. Salas

Final Report

16. Abstract

A numerical procedure has been developed to compute the inviscid super/hypersonic flow fields about complex vehicle geometries accurately and efficiently. A second-order accurate finite difference scheme is used to integrate the three-dimensional Euler equations in regions of continuous flow, while all shock waves are computed as discontinuties via the Rankine-Hugoniot jump conditions. Conformal mappings are used to develop a computational grid. The effects for equilibrium air are included using curve fits of Mollier charts. All the aforementioned procedures have been reported in detail in previous reports. This report deals only with modifications to these procedures in four specific areas: inlet mass ingestion, subsonic axial Mach number, improved conformal mappings, and vehicles flying at yaw. In each area both the modifications to the computational procedures and computer code are discussed.

17. Key Words (Suggested by Author(s))	18. Distribution Statement
Vehicle flow fields Three-dimensional flows supersonic/hypersonic flows inviscid flows numerical calculations	Unclassified - Unlimited Subject Category 02

19. Security Classif. (of this report)	20. Security Classif. (of this page)	21. No. of Pages	22. Price*
Unclassified	Unclassified	27	$4.50

* For sale by the National Technical Information Service, Springfield, Virginia 22161

NASA-Langley, 1979